A novel role for HMGB1 in TLR9-mediated inflammatory responses to CpG-DNA

Stanimir Ivanov,[1] Ana-Maria Dragoi,[1] Xin Wang,[1] Corrado Dallacosta,[2] Jennifer Louten,[1] Giovanna Musco,[2] Giovanni Sitia,[2] George S. Yap,[1] Yinsheng Wan,[3] Christine A. Biron,[1] Marco E. Bianchi,[4] Haichao Wang,[5] and Wen-Ming Chu[1]

[1]Department of Molecular Microbiology and Immunology, Brown University, Providence, RI; [2]San Raffaele Scientific Institute, Milano, Italy; [3]Department of Biology, Providence College, Providence, RI; [4]San Raffaele University, Faculty of Medicine, Milano, Italy; [5]Department of Emergency Medicine, North Shore-Long Island Jewish Research Institute, Manhasset, NY

CpG-DNA or its synthetic analog CpG-ODN activates innate immunity through Toll-like receptor 9 (TLR9). However, the mechanism of TLR9 activation by CpG-DNA remains elusive. Here we have identified HMGB1 as a CpG-ODN–binding protein. HMGB1 interacts and preassociates with TLR9 in the endoplasmic reticulum-Golgi intermediate compartment (ER-GIC), and hastens TLR9's redistribution to early endosomes in response to CpG-ODN. CpG-ODN stimulates macrophages and dendritic cells to secrete HMGB1; in turn, extracellular HMGB1 accelerates the delivery of CpG-ODNs to its receptor, leading to a TLR9-dependent augmentation of IL-6, IL-12, and TNFα secretion. Loss of HMGB1 leads to a defect in the IL-6, IL-12, TNFα, and iNOS response to CpG-ODN. However, lack of intracellular TLR9-associated HMGB1 can be compensated by extracellular HMGB1. Thus, the DNA-binding protein HMGB1 shuttles in and out of immune cells and regulates inflammatory responses to CpG-DNA. (Blood. 2007;110:1970-1981)

Introduction

Members of the TLR family mediate the innate immune response upon encounter with biochemically diverse pathogen molecules.[1,2] Among them is TLR9, which is essential for recognition of microbial CpG-DNA or its analog, synthetic oligonucleotides containing a CpG motif (CpG-ODNs).[3-6] CpG-DNA/CpG-ODNs activate macrophages, monocytes, and dendritic cells (DCs) to secrete proinflammatory cytokines, driving the Th1 response[3-6] and serving as attractive adjuvants in vaccine strategies for allergy, asthma, infectious disease, and cancer. TLR9 is confined primarily to cells of the immune system and is not present on the cell surface.[7-10] It is proposed that TLR9 is initially localized in the endoplasmic reticulum (ER), and redistributes to early endosomes upon stimulation with CpG-DNA.[9,11,12] TLR9 becomes activated and recruits MyD88,[9,11,12] leading to subsequent immune responses. However, the mechanism by which TLR9 is activated remains elusive, and it is unknown whether CpG-DNA-binding proteins are involved in this activation process.

HMGB1 is an abundant, highly conserved nuclear protein that modulates chromatin structure, facilitates interaction of proteins with DNA, regulates transcription, and assists in V(D)J recombination.[13,14] Immune cells stimulated with IFNγ, IL-1, and TNFα export nuclear HMGB1 to the cytoplasm and subsequently secrete it.[15] HMGB1 can also be passively released by necrotic cells,[16] serving as a signal for trauma and tissue damage.[17] Additionally, HMGB1 is released during bacterial or viral infection,[18,19] and extracellular HMGB1 can act as a chemoattractant for inflammatory cells, strongly suggesting its role as a modulator of the immune system.

In this study, we demonstrate that CpG-ODN–treated macrophages and DCs quickly secrete HMGB1; moreover, HMGB1 engages CpG-ODNs and enhances their immunostimulatory potential in a TLR9-dependent manner. Confocal microscopy reveals that HMGB1 preassociates with TLR9 and colocalizes with markers of the ER, the ERGIC, and the Golgi in quiescent cells. Upon stimulation with CpG-ODN, HMGB1 and TLR9 colocalize with the early endosomal marker EEA1. Ablation or depletion of HMGB1 impaired redistribution of TLR9 to early endosomes in response to CpG-ODN. As a consequence, HMGB1-deficient cells exhibited substantially decreased responses to CpG-ODN, but these defects could be complemented by extracellular HMGB1.

Materials and methods

Animals

Myd88$^{-/-}$, *Tlr2*$^{-/-}$, *Tlr9*$^{-/-}$, and their control littermates on B6/129 genetic background were gifts from Dr Akira and bred at Brown University (Providence, RI). *Hmgb1*$^{+/-}$ mice were bred at San Raffaele, Italy. C.C3-*Tlr4*$^{lps\text{-}d/J}$ and their control were purchased from the Jackson Laboratory (Bar Harbor, ME). All institutions followed the respective national and local regulations on animal experimentation. Bone marrow–derived macrophages (BMDMs) and bone marrow–derived DCs (BMDCs) were prepared as previously described.[7,9,10,20]

Oligodeoxynucleotides and antibodies

Endotoxin-free CpG-ODN 1018 and GpG-ODN 1019 were synthesized with a phosphorothioate backbone (Trilinker, San Diego, CA). For binding and microscopy studies, all ODNs (1018, 1019, 1668, and n1668) containing Cy5 (Sigma, St Louis, MO) or biotin (Invitrogen, San Diego, CA) at the 3′ end were synthesized on the phosphodiester backbone. CpG-A (2216) was purchased from InvivoGen (San Diego, CA).

Antibodies used were as follows: anti-HMGB1 (mouse monoclonal [MBL International, Nagoya, Japan]; rabbit polyclonal [PharMingen, San

Submitted August 31, 2006; accepted May 28, 2007. Prepublished online as *Blood* First Edition paper, June 4, 2007; DOI 10.1182/blood-2006-09-044776.

The online version of this article contains a data supplement.

The publication costs of this article were defrayed in part by page charge payment. Therefore, and solely to indicate this fact, this article is hereby marked "advertisement" in accordance with 18 USC section 1734.

Diego, CA]); anti-TLR9 (monoclonal and polyclonal; Imgenex, San Diego, CA); anti-EEA1, anti-ERGIC-53, anticalnexin and anti-GM130 (goat polyclonal; Santa Cruz Biotech, Santa Cruz, CA); and AlexaFluore- and FITC/rhodamine-conjugated secondary antibodies (Molecular Probes [Eugene, OR] and Biosource [Camarillo, CA], respectively).

ELISA analysis

Macrophages and DCs were seeded ($0.8\text{-}2.5 \times 10^5$/well) in triplicate in 96-well plates and treated with endotoxin-free poly(I:C) (GE Healthcare, Piscataway, NJ), CpG-ODN (1018), CpG-A (2216), GpG-ODN (1019), LPS (Sigma), or PGN (Sigma) in the presence or absence of recombinant HMGB1 (rHMGB1), produced by HMGBiotech (Milan, Italy) and purified from *E coli* (LPS $<$ 4 EU per mg). The LPS inhibitor polymyxin B (10 μg/mL; Sigma) was added for at least 15 minutes prior to treatment. After 24 hours in culture, supernatants were collected and assayed for IL-6, IL-12, and TNFα with enzyme-linked immunosorbent assay (ELISA) kits (PharMingen).

Confocal microscopy

Cells were seeded at 7.5×10^4 per chamber on culture slides. Following treatments, cells were fixed with 3% paraformaldehyde, permeabilized with 0.2% Triton X-100 in PBS for 5 minutes, and stained with antibodies (1:300 dilution for rabbit anti-HMGB1, mouse anti-TLR9, goat anticalnexin, and anti-ERGIC; 1:200 for goat anti-GM130). An inverted Leica TCS SP2 AOBS confocal microscope (DMIRE2; Wetzlar, Germany) with a HC × PL APO lbd. BL 63×/1.4 oil immersion objective was used. Fluorophores were sequentially excited at 488, 543, and 633 nm to prevent cross-excitation. Images were collected and raw data were quantified with Leica Imaging Software (CTRMIC; TCS SP2). Representative images were processed in Photoshop (Adobe Systems, San Jose, CA) applying only linear corrections.[13,21,22]

Immunoprecipitation and immunoblotting

Following treatment, whole-cell lysates (WCLs) were prepared with a lysis buffer.[23] To examine protein interactions, WCLs (400 μg) were incubated with 0.5 μg anti-HMGB1 (polyclonal) or anti-TLR9 (monoclonal) antibodies and 20 μL protein A/G-beads at 4°C overnight. After several washings with lysis buffer, proteins were boiled and separated on sodium dodecyl sulfate-polyacrylamide gel electrophoresis (SDS-PAGE) and subsequently probed with anti-TLR9 (monoclonal) or anti-HMGB1 (monoclonal) antibodies. Visualization was completed with enhanced chemiluminescence (ECL; GE Healthcare).

Derivation of HMGB1-deficient and wt cells

Hmgb1 heterozygotes were on pure BALB/C genetic background ($>$ 10 backcrosses). *Hmgb1*$^{-/-}$ embryos were significantly fewer (6%) than expected by Mendelian segregation, contrary to what is described for mixed genetic backgrounds.[24] Fetal livers were taken from sibling 14-day embryos; they were dissociated with a cell strainer, and cells were either expanded for 8 days to differentiate into DCs and macrophages[25] or infected with a retrovirus coding for HoxB4 and puromycin resistance. Pools of puromycin-resistant cells were expanded in IMDM + 10% FBS in the presence of IL-3 (10 ng/mL), IL-6 (10 ng/mL), and stem-cell factor (20 ng/mL), and further cultured in the presence of GM-CSF (5 ng/mL) for 7 days (DCs) or BMDM medium for 10 days (macrophages) prior to treatments.

Flow cytometry

Cell-surface staining on DCs derived from immortalized fetal liver progenitor cells (IFLDCs), DCs derived from primary fetal liver progenitor cells (PFLDCs), macrophages derived from immortalized fetal liver progenitor cells (IFLDMs), and macrophages derived from primary fetal liver progenitor cells (PFLDMs) was performed in PBS + 2% FBS with fluorescently conjugated antibodies against CD11c, CD11b, and F4/80 (eBiosciences, San Diego, CA); for CpG-ODN/GpG-ODN endocytosis by IFLDCs, cells were treated with CpG-ODNs labeled with TOTO-3 (Molecular Probes), or with Cy5-CpG-ODN/GpGp-ODN for the indicated time points. Cells were extensively washed, trypsinized, washed again, and then fixed in 2% paraformaldehyde. Data were immediately acquired using a FACSCalibur (Becton Dickinson, Mountain View, CA) and analyzed using Cell Quest Pro software, version 5.2 (Becton Dickinson).

Results

HMGB1 is a CpG-DNA–binding protein

IFNγ can sensitize primary murine macrophages to produce cytokines in response to CpG-DNA.[7,9,10] Although IFNγ is able to alter the level of TLR9 protein,[9] the possibility that IFNγ induces secretion of other protein factors enhancing the CpG-DNA response has yet to be explored. To search for such factors, serum-free media from IFNγ-treated Raw264.7 cells were fractionated on a single-stranded DNA column followed by incubation with CpG-ODN-biotin and precipitation with streptavidin agarose. Bound proteins were separated by SDS-PAGE, silver stained, and subjected to mass spectrometry. This identified HMGB1 as a CpG-ODN–binding protein (Figure 1A).

Generally, CpG-ODNs fall in 2 groups: class A and class B. The former, which mainly elicits IFNα/β production, contains a single CpG motif and a poly-G tail at the 3′ end on a mixed phosphorothioate-phosphodiester backbone (eg, D-19).[26-28] The latter, which activates DCs and macrophages to produce inflammatory cytokines, contains single or multiple CpG motifs on a phosphorothioate backbone (eg, 1018, 1668).[26] To address the binding specificity of HMGB1 to CpG-ODNs, we precipitated recombinant HMGB1 (rHMGB1)[17] or histone H2A using biotin-labeled ODNs. Interestingly, CpG-ODNs (D-19, 1018, and 1668) precipitated 3- to 8-fold higher amounts of rHMGB1 than their control GpG/GpC-ODNs (c-405, 1019, and n-1668)[29-31] (Figure 1B). In contrast, all the tested ODNs bound histone H2A equally well (Figure 1B). To further confirm the binding preference of HMGB1 for CpG-ODNs, we determined circular dichroism (CD) spectra of ODNs in the presence or absence of HMGB1. Incubation of CpG-ODN 1018, but not GpG-ODN 1019, with rHMGB1 led to a dramatic change in the CD spectra of the ODN (Figure 1C), suggesting that HMGB1 can bind to single-stranded DNA with some preference for CpG-ODNs over GpG-ODN.

HMGB1 augments inflammatory cytokine responses to CpG-ODN in a TLR9-dependent manner

The effect of CpG-ODN on HMGB1 secretion has been investigated before, with conflicting results.[32,33] When we tested whether CpG-ODN 1018 (simply called CpG-ODN) induces secretion of HMGB1 in bone marrow–derived DCs (BMDCs) and macrophages (BMDMs), we found that it triggered HMGB1 release within minutes (Figure 2A), rather than after several hours as reported for LPS, IFNγ, or TNFα.[21,22] This release was not due to cell death as indicated by a lack of LDH release, a marker for cell necrosis (Figure 2A), and also by an observed cell survival rate of 95% to 99%. Because HMGB1 can recognize CpG-ODNs, its presence in the environment could potentially regulate the response to CpG-DNA. We treated BMDMs with CpG-ODN together with the LPS inhibitor polymyxin B in the presence or absence of rHMGB1. CpG-ODN together with rHMGB1 was more effective in eliciting IL-6 secretion compared with CpG-ODN alone or HMGB1 alone (Figure 2B). The response to CpG-ODN plus HMGB1 was greater than the sum of the responses to CpG-ODN and HMGB1

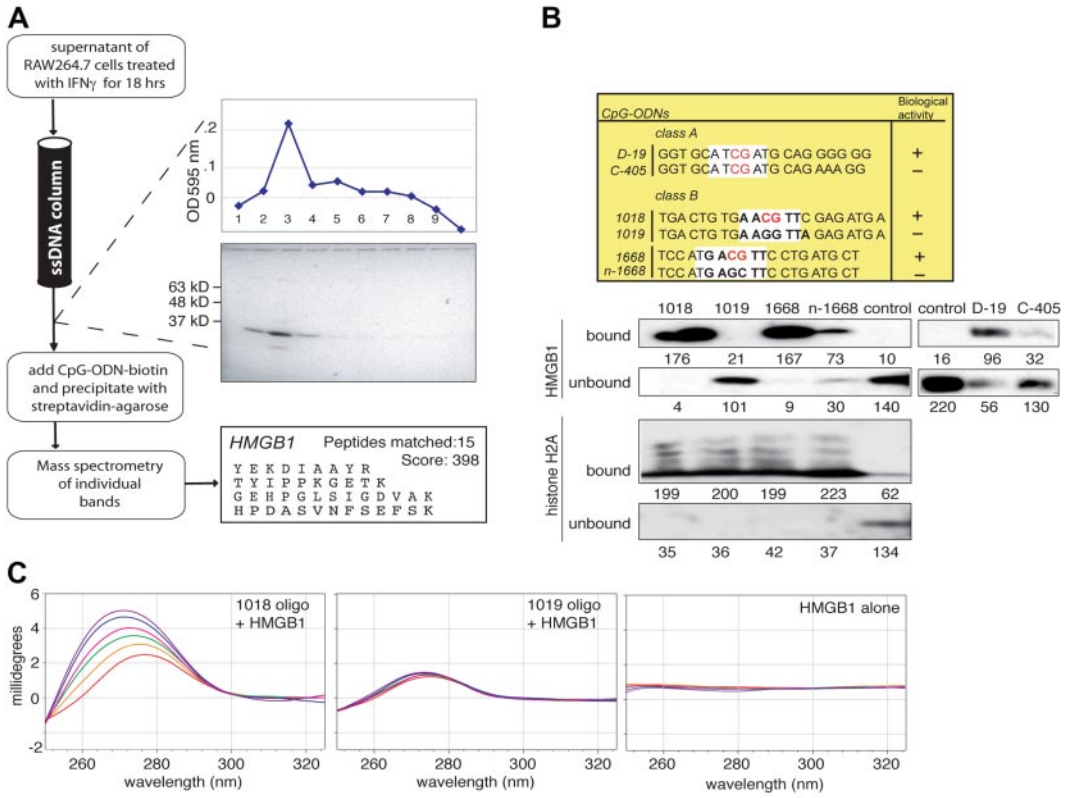

Figure 1. The DNA-binding protein HMGB1 is a CpG-DNA engaging factor released by macrophages in response to IFNγ. (A) Purification of HMGB1 as a CpG-DNA–binding protein. Raw264.7 cells (2.5×10^6/mL) were treated with IFNγ (30 ng/mL) for 18 hours. Cell-free supernatants (50 mL) were slowly loaded (10 mL/hour) onto a single-stranded DNA-cellulose column pre-equilibrated with buffer A (20 mM Tris-Cl, pH 8.8, 50 mM NaCl, 1 mM EDTA, 1 mM DTT, 5% glycerol). After absorption, the column was washed sequentially with 150 mL buffer A and rinsed with 150 mL 0.1 M NaCl in buffer A. Proteins were recovered from the column by sequential elution with 0.5 and 2 M NaCl in buffer A. Fractions (1 mL) were dialyzed overnight against buffer B (5 mM KH_2PO_4/NaOH, pH 7.9, 10% glycerol). Of each fraction, 30 μL was loaded on a 10% SDS-PAGE and subsequently silver stained. Fractions 2, 3, and 4 that had peak protein content were pooled, diluted with buffer A at 0.16 M NaCl, and incubated with 0.1 mg biotinyl-1018 ODN for 30 minutes followed by incubation overnight at 4°C with 0.5 mL streptavidin-agarose beads. The beads were washed with buffer A containing 0.16 M NaCl, boiled, and loaded on a 10% SDS-PAGE, and proteins were detected by silver staining. All visible bands were excised and subjected to mass spectrometry. Several representative HMGB1 peptides are listed. (B) HMGB1 binds CpG-ODNs (1018, 1668, and D-19) preferentially over controls (1019, n-1668, and c-405). Mouse rHMGB1 (25 ng) or histone H2A (25 ng) was incubated in the absence (control) or presence of CpG-ODN-biotin (5 μg) for 60 minutes. ODNs were immunoprecipitated with streptavidin-agarose beads, washed, and subjected to immunoblot analysis (IB) with anti-HMGB1 antibody. The levels of unbound HMGB1 or H2A were estimated by collecting 5% of the supernatant from each precipitation reaction. The gray value of the pixel intensity (range, 1 to 250) of the respective protein bands is listed. Results represent 1 of 6 or 3 reproducible independent experiments for HMGB1 and H2A binding, respectively. (C) CD spectra of oligos 1018 and 1019 in the presence of increasing amounts of HMGB1. All spectra have been acquired at 20°C, 20 mM phosphate buffer, pH 7.0, 10 mM NaCl, with an initial DNA concentration of 10 μM. Traces from red to violet correspond to the spectra acquired by adding 0, 1, 2, 2.8, 4.5, or 10 μM protein to the oligo solutions. The spectra were corrected by subtracting the buffer and the protein, and compensating for dilution. The panel "HMGB1 alone" shows the spectra recorded for 0, 1, 2, 2.8, 4.5, or 10 μM protein (in the same buffer and in the absence of DNA), to show that corrections applied to the recorded spectra are neutral in the wavelength range considered here.

added separately. In contrast, the addition of rHMGB1 failed to augment IL-6 production in BMDMs in response to PGN (2.5 μg/mL) and LPS (0.01, 0.1, 0.2, or 1 μg/mL) (Figure 2B, and data not shown). HMGB1 also enhanced the secretion of IL-6, IL-12, and TNFα in response to CpG-ODN in BMDCs (Figure 2C).

This phenomenon was strictly dependent on the TLR9/MyD88 pathway, which is essential for cytokine induction by CpG-ODN.[7] TLR9 inhibitors chloroquine and quinacrine (data not shown) and the loss of TLR9 or MyD88 severely impaired IL-6 production in BMDMs in response to CpG-ODN, regardless of the presence or absence of rHMGB1 (Figure 2D upper panel). Conversely, the lack of functional TLR4 or the deletion of TLR2 did not significantly affect the ability of HMGB1 to augment cytokine secretion in response to CpG-ODNs (Figure 2D lower panel). Together, our findings demonstrate that HMGB1 specifically enhances CpG-DNA-triggered cytokine responses that are TLR9 dependent.

Unexpectedly, the amount of endocytosed CpG-ODN was moderately decreased when CpG-ODN was added together with rHMGB1 (Figure 2E). This suggests that the augmentation by HMGB1 of cytokine responses to CpG-ODN is not due to increased CpG-DNA uptake by cells. We hypothesized that HMGB1 enhances the association of CpG-ODN with TLR9 intracellularly. Thus, we examined the kinetics of CpG-ODN association with TLR9. CpG-ODN was used to treat WEHI 231, a murine B-lymphoma cell line that responds to CpG-DNA by producing cytokines.[34] TLR9 was immunoprecipitated and its association to CpG-ODN was determined by a specific polymerase chain reaction (PCR) analysis (Figure S1, available on the *Blood* website; see the Supplemental Figures link at the top of the online article). Following CpG-ODN addition to the medium, we detected a transient association between TLR9 and CpG-ODNs, which peaked at 60 minutes after treatment (Figure 2F). In the presence of HMGB1, the maximum association of CpG-ODN with TLR9 occurred within 15 to 30 minutes (Figure 2G). These results suggest that extracellular HMGB1 accelerates the formation of the CpG-DNA/TLR9 complex.

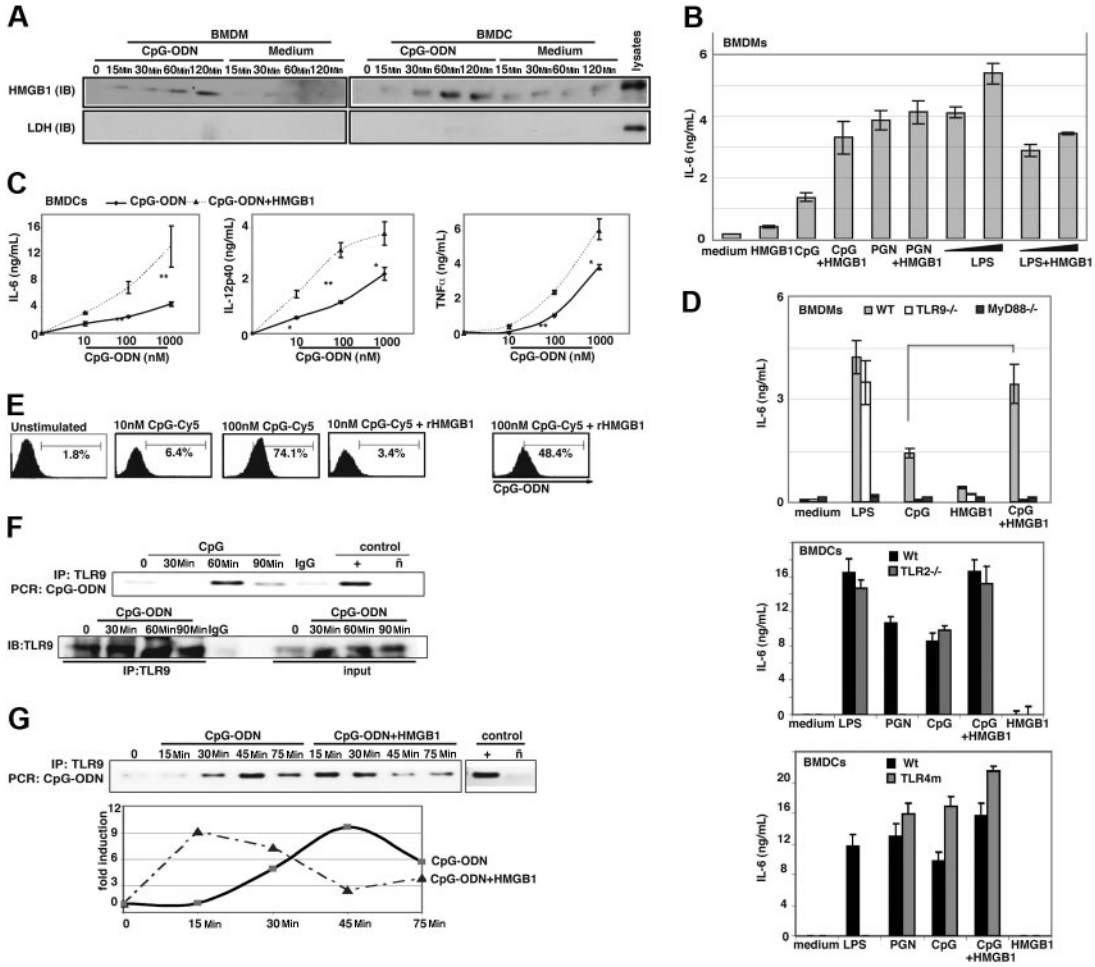

Figure 2. HMGB1 potentiates the cytokine response to CpG-ODNs. (A) CpG-ODN triggers the release of HMGB1. BMDCs (3×10^6 cells/mL) and BMDMs (2×10^6 cells/mL) were treated with CpG-ODN (10 μg/mL) for the indicated time periods. The medium bathing the cells (40 μL) was subjected to SDS-PAGE and immunoblotted (IB) with anti-HMGB1 or anti-LDH antibody. As a positive control, 2 μg macrophage whole cell lysates were used. Cell viability was determined by trypan blue exclusion. (B-D) Extracellular HMGB1 enhances induction of cytokines by CpG-DNA in a TLR9-dependent manner. Cells were seeded at 1 to 2.5×10^5/well in a 96-well plate (in triplicate) and then treated with CpG-ODN, PGN, or LPS, or left untreated. The LPS inhibitor polymyxin B (10 μg/mL) was used in all treatments except LPS. (B) BMDMs were treated with CpG-ODN (10 μg/mL), LPS (0.2 or 1 μg/mL), or PGN (2.5 μg/mL) in the presence or absence of rHMGB1 (50 ng/mL), or left untreated for 24 hours. IL-6 secretion was assessed by ELISA (averages of triplicates ± SD). Experiments were replicated 3 times. (C) BMDCs were treated with CpG-ODN (10 nM to 1000 nM) in the presence or absence of rHMGB1 (1 μg/mL) or left untreated for 24 hours. Levels of IL-6, IL-12, and TNFα secretion were assessed by ELISA (averages of triplicates ± SD). Experiments were replicated 3 times. (D, upper panel) BMDMs from wild-type (wt), *Tlr9*$^{-/-}$, or *Myd88*$^{-/-}$ mice were treated for 24 hours with LPS (0.2 μg/mL), CpG-ODN (10 μg/mL) plus or minus rHMGB1 (50 ng/mL), or rHMGB1 alone (50 ng/mL); IL-6 secretion was assessed by ELISA. Bars represent the average of 6 independent experiments done in triplicate plus or minus SD (**$P < .001$, Student *t* test). (D, lower panels) BMDCs from wt, *Tlr4m,* or *Tlr2*$^{-/-}$ mice were treated with LPS (0.1 μg/mL), PGN (10 μg/mL), or CpG-ODN (10 μg/mL) plus or minus rHMGB1 (50 ng/mL). IL-6 secretion was assessed by ELISA. (E) rHMGB1 does not effect CpG-ODN uptake by BMDCs. Cells were treated with CpG-ODN-Cy5 in the presence or absence of rHMGB1 (250 ng/mL) for 1 hour as indicated. Cells were trypsinized and Cy5-positive cells were determined by fluorescence-activated cell sorting (FACS) analysis. (F) TLR9 was immunoprecipitated from the lysates of WEHI-231 cells that were treated with CpG-ODN (10 μg/mL). The presence of CpG-ODN in the TLR9 immunoprecipitate (IP) was detected by PCR. Levels of immunoprecipitated TLR9 for each reaction were assessed by immunoblotting (IB). (G) rHMGB1 speeds up the formation of the CpG-ODNs/TLR9 complex. WEHI-231 cells were treated with CpG-ODN (10 μg/mL) alone or preincubated for 1 hour with rHMGB1 (50 ng). TLR9 was immunoprecipitated and the levels of CpG-ODN in the TLR9 complex were assessed by PCR.

HMGB1 and TLR9 form a complex within specialized vesicles

Since HMGB1 engages CpG-ODNs, and CpG-ODNs engage TLR9, we examined the possible interaction of HMGB1 with TLR9. WEHI-231 cells were treated with CpG-ODN and the association of TLR9 with HMGB1 was assessed by immunoprecipitation. Surprisingly, we found that HMGB1 preassociated with TLR9 prior to CpG-ODN treatment (Figure 3A left panel). We examined the specificity of this interaction in splenocytes, which express the highest levels of TLR9 among cells and tissues.[7] As shown in Figure 3A (right panel), HMGB1 was detected in TLR9 complexes immunoprecipitated from wt, but not TLR9-deficient, splenocytes.

The observed HMGB1/TLR9 association in quiescent cells was puzzling because HMGB1 is predominantly a nuclear protein, whereas TLR9 has been reported to reside in the ER and translocate to endosomes after CpG-ODN stimulation.[11,35] In order to reconcile where the TLR9/HMGB1 complex resides in BMDMs, we used confocal microscopy. Although dispersed TLR9 staining was evident, high levels of TLR9 were detected in discrete vesicular structures prior to CpG-ODN treatment (Figure 3B,C and Figure S2C,D). As previously described,[11] in wt BMDMs, within 5 minutes of stimulation, Cy5-labeled CpG-ODN distinctively colocalized with TLR9 in vesicular structures, most likely early endosomes, followed by translocation into the tubular lysosomal

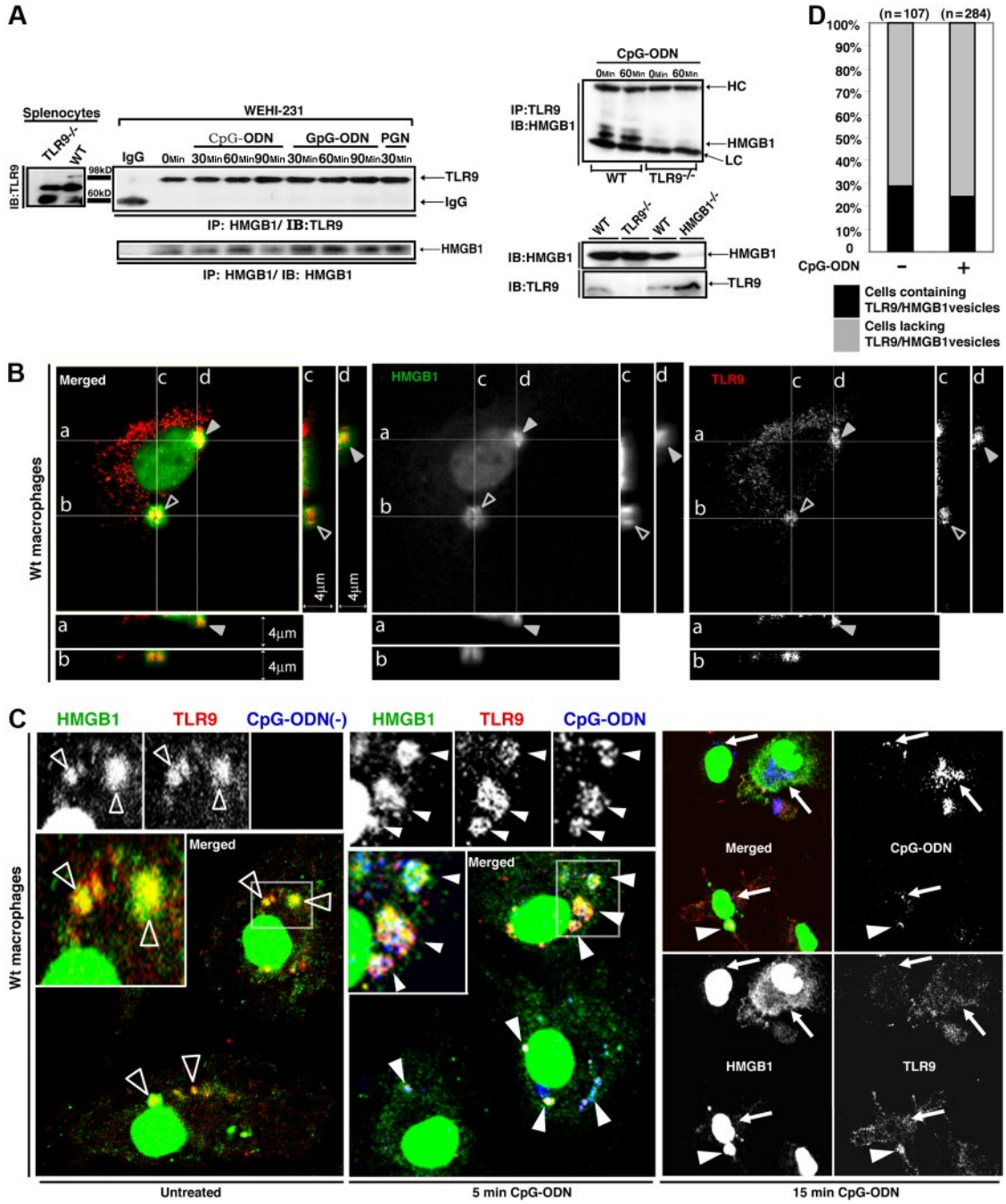

Figure 3. BMDMs contain vesicles rich in HMGB1 and TLR9, which participate in CpG-ODN recognition. (A) HMGB1 is associated with TLR9 prior to CpG-ODN treatment. Lysates from TLR9-deficient and wt splenocytes were used to identify the TLR9 band (left panel). WEHI-231 cells were treated with CpG-ODN (10 μg/mL), GpG-ODN (10 μg/mL), or peptidoglycan (PGN, 10 μg/mL) for the times indicated. HMGB1 was immunoprecipitated from cell lysates, and the presence of TLR9 or HMGB1 in the precipitated materials was detected by IB (left panel). Wt and TLR9-deficient splenocytes were treated with CpG-ODN (10 μg/mL) for the indicated time points or left untreated (top right panel). TLR9 was immunoprecipitated, and coprecipitation of HMGB1 with TLR9 was determined by IB. Whole-cell lysates from wt, HMGB1-deficient, and TLR9-deficient cells were probed by anti-HMGB1 and anti-TLR9 antibodies (bottom right panel). (B) Confocal microscopy of quiescent BMDMs reveals that HMGB1 and TLR9 colocalize in vesicular structures (indicated by triangles in z-stack images), which consistently appear close to the nucleus. Depth sections across 2 vesicles are shown in i-iv. Proteins were detected with anti-HMGB1/FITC and anti-TLR9/rhodamine. (C) BMDMs treated with CpG-ODN-Cy5 (1018, 5 μg/mL) as indicated were fixed, permeabilized, and stained with anti-TLR9/rhodamine and anti-HMGB1/FITC. △ indicate HMGB1/TLR9-containing vesicles; ▲ indicate CpG-DNA–containing vesicles. Solid arrows point to dispersed CpG-ODN-Cy5 staining in the tubular lysosomal compartment. (D) Quantification of the percentage of BMDMs containing at least one TLR9/HMGB1 vesicle. Cells were treated or not with CpG-ODN (1018, 5 μg/mL) in at least 3 independent experiments. Vesicles clearly visible within a single plane were counted.

compartment (Figure 3C). We observed that these CpG-ODN–containing endosomes acquired both TLR9 and HMGB1 simultaneously (Figure 3C). Approximately 29% of optical sections across cells contained TLR9/HMGB1 vesicles, and this percentage remained relatively unchanged following CpG-ODN exposure (Figure 3D). However, this number represents an underestimation as it accounts for only a single plane of vision.

Taken together, immunoprecipitation and immunofluorescence experiments indicate that HMGB1 specifically associates with TLR9, before and during the association of CpG-ODN to TLR9.

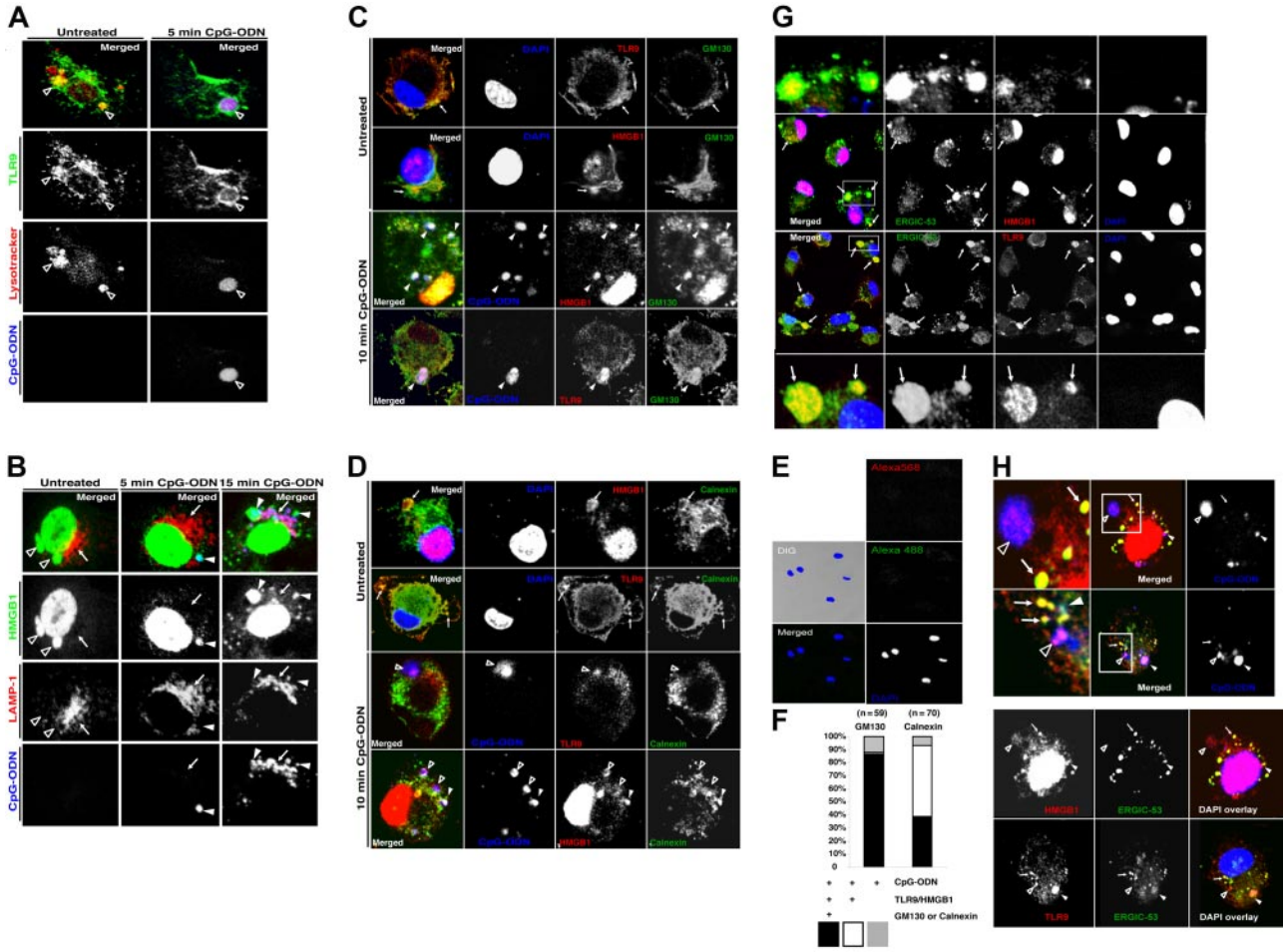

Figure 4. The HMGB1/TLR9-containing vesicles colocalize with calnexin, GM130, and ERGIC-53, but lack lysosomal markers. (A) TLR9-containing vesicles accumulated the acidophilic fluorophore LysoTracker. BMDMs were treated with LysoTracker for 30 minutes prior to stimulation with CpG-ODNs (5 μg/mL), then fixed, permeabilized, and stained with anti-TLR9/FITC. Open triangles indicate representative vesicles. (B) BMDMs were stained with anti-HMGB1/FITC and anti-LAMP-1/rhodamine following stimulation with CpG-ODNs (5 μg/mL). △ indicate HMGB1-containing vesicles; ▲, CpG-DNA-containing vesicles; and ↑, tubular lysosomal compartment. (C-D) BMDMs were stained with anti-GM130/Alexa488 (C) or anti-calnexin/Alexa488 (D) and anti-TLR9/Alexa568 or anti-HMGB1/Alexa568, prior to or following stimulation with CpG-ODN-Cy5 (5 μg/mL) for 10 minutes. Confocal images were acquired by indirect immunofluorescence. Solid arrows indicate colocalization between GM130/calnexin and TLR9 or GM130 and HMGB1. Solid triangles indicate vesicles containing CpG-ODN-Cy5 as well as GM130 and TLR9 or HMGB1. Open triangles indicate vesicles containing HMGB1/TLR9 and CpG-ODN but lack calnexin or GM130. (E) Control staining of BMDMs with antimouse-Alexa568/antirabbit-Alexa568 and antigoat-Alexa488. (F) Percentages of vesicles containing CpG-ODNs alone, CpG-ODN in the presence of TLR9/HMGB1, or CpG-ODN in the presence of TLR9/HMGB1 and GM130 or calnexin. Vesicles were analyzed from 2 independent experiments. (G,H) Quiescent (G) or treated (H) BMDMs were stained with anti-ERGIC-53/Alexa488 and either anti-TLR9/Alexa568 or anti-HMGB1/Alexa568. Rectangular regions showing representative colocalization between ERGIC-53/TLR9 and ERGIC/HMGB1 (solid arrows) are magnified. Colocalization of CpG-ODNs with TLR9/HMGB1 in the presence or absence of ERGIC-53 is shown with solid or open triangles, respectively.

HMGB1/TLR9-containing vesicles contain calnexin, GM130, and ERGIC-53 but lack lysosomal resident proteins

The TLR9 inhibitors chloroquine and quinacrine are weak bases and preferentially partition to acidic vesicles,[36,37] suggesting that TLR9 activation requires an acidic environment. Thus, we sought to determine when TLR9 first encounters such an acidic environment. The acidotropic fluorescent probe LysoTracker (Molecular Probes, Eugene, OR) was allowed to accumulate in BMDMs prior to CpG-ODN stimulation. Unexpectedly, the vesicles containing TLR9 and HMGB1 appeared to be acidic prior to CpG-ODN stimulation (Figure 4A), suggesting that they might represent a population of secretory lysosomes,[38] or could belong to acidic intracellular compartments such as the trans-Golgi network and the ER-Golgi intermediate compartment (ERGIC).[39] However, the lysosome-associated membrane protein 1 (LAMP-1), a hallmark of both regular and secretory lysosomes,[38,40] did not colocalize with HMGB1 prior to or during early stages of CpG-ODN endocytosis, but only 15 minutes after stimulation (Figure 4B). This is consistent with a previous report that CpG-ODNs at late stages accumulate in the tubular lysosomal compartment.[11] These observations suggest that the vesicles containing HMGB1 and TLR9 are not lysosomes.

Next, we tested the possibility that TLR9- and HMGB1-contaning vesicles belong to the Golgi network. Both a *cis*-Golgi resident transmembrane protein GM130 and an ER marker calnexin colocalized with TLR9 and HMGB1 in quiescent macrophages (Figure 4C,D). Five minutes after stimulation, a survey of 129 cells showed that approximately 10% of the endocytosed CpG-ODN localized in vesicles that lacked TLR9/HMGB1, suggesting that the TLR9/HMGB1 vesicles do not participate in CpG-DNA endocytosis. About 87% of TLR9/HMGB1/GM130-containing vesicles colocalized with CpG-ODNs (Figure 4F). However, only about 40% of the TLR9/HMGB1/calnexin-containing vesicles colocalized with CpG-ODNs (Figure 4D,F). These results suggest that acquisition of CpG-ODNs by the TLR9/HMGB1-containing vesicles leads to remodeling of the organelle's membrane, as GM130 is retained but calnexin is rapidly lost.

More specifically, we investigated whether HMGB1/TLR9 are located in the ERGIC. The transmembrane chaperone ERGIC-53,

which accumulates within the ERGIC and serves as its marker,[41] colocalized with TLR9 and HMGB1 in assorted or clusters of vesicles within quiescent BMDMs (Figure 4G). These vesicles were observed in the perinuclear region and in the cell periphery, consistent with the dynamic nature of the ERGIC.[42] Following CpG-ODN endocytosis, TLR9/HMGB1 vesicles devoid of DNA exhibited a more robust staining for ERGIC-53 compared with those vesicles containing DNA (Figure 4H).

Taken together, these results indicate that HMGB1- and TLR9-containing vesicles are acidic and colocalize with markers of the ER, the ERGIC, and Golgi in quiescent cells, and suggest that they may belong to the ERGIC.

HMGB1 in the TLR9- and ERGIC-containing vesicles originates from the nucleus and can be reacquired from the extracellular milieu

Although HMGB1 is mainly nuclear, both active and passive transport ferry it into the cytoplasm.[43] Two nuclear export sequences on HMGB1 govern its nuclear export via the chromosome region maintenance 1 protein (CRM1), also known as exportin-1.[43] Leptomycin B (LMB) can bind directly to CRM1, thus blocking interaction with its targets.[44,45] To determine whether HMGB1 that colocalizes with TLR9 and ERGIC-53 originates from the nucleus, we treated BMDMs with LMB for 45 minutes. As shown in Figure 5A,B, in the presence of LMB HMGB1 was not predominantly associated with vesicles that contained TLR9. As a result, the HMGB1/TLR9 complex failed to assemble as verified by an immunoprecipitation assay (Figure 5C). Interestingly, the TLR9-contaning vesicles depleted of HMGB1 by LMB regained HMGB1 when rHMGB1 was added in the medium (compare Figure 5D with 5A). Further, in HMGB1-deficient macrophages (described in one of the following sections), addition of rHMGB1 to the medium dramatically increased colocalization of HMGB1 with TLR9 (Figure 5E).

Similarly, the original source of HMGB1 that colocalized with ERGIC-53 was found to be the nucleus, as 60 minutes of treatment with LMB led to an almost complete depletion of HMGB1 in the cytoplasm in the presence or absence of CpG-ODN, and no colocalization of HMGB1 with ERGIC-53 was observed (Figure 5F). Addition of exogenous HMGB1 reconstituted its colocalization with ERGIC-53 (Figure 5F). Therefore, HMGB1 can enter the

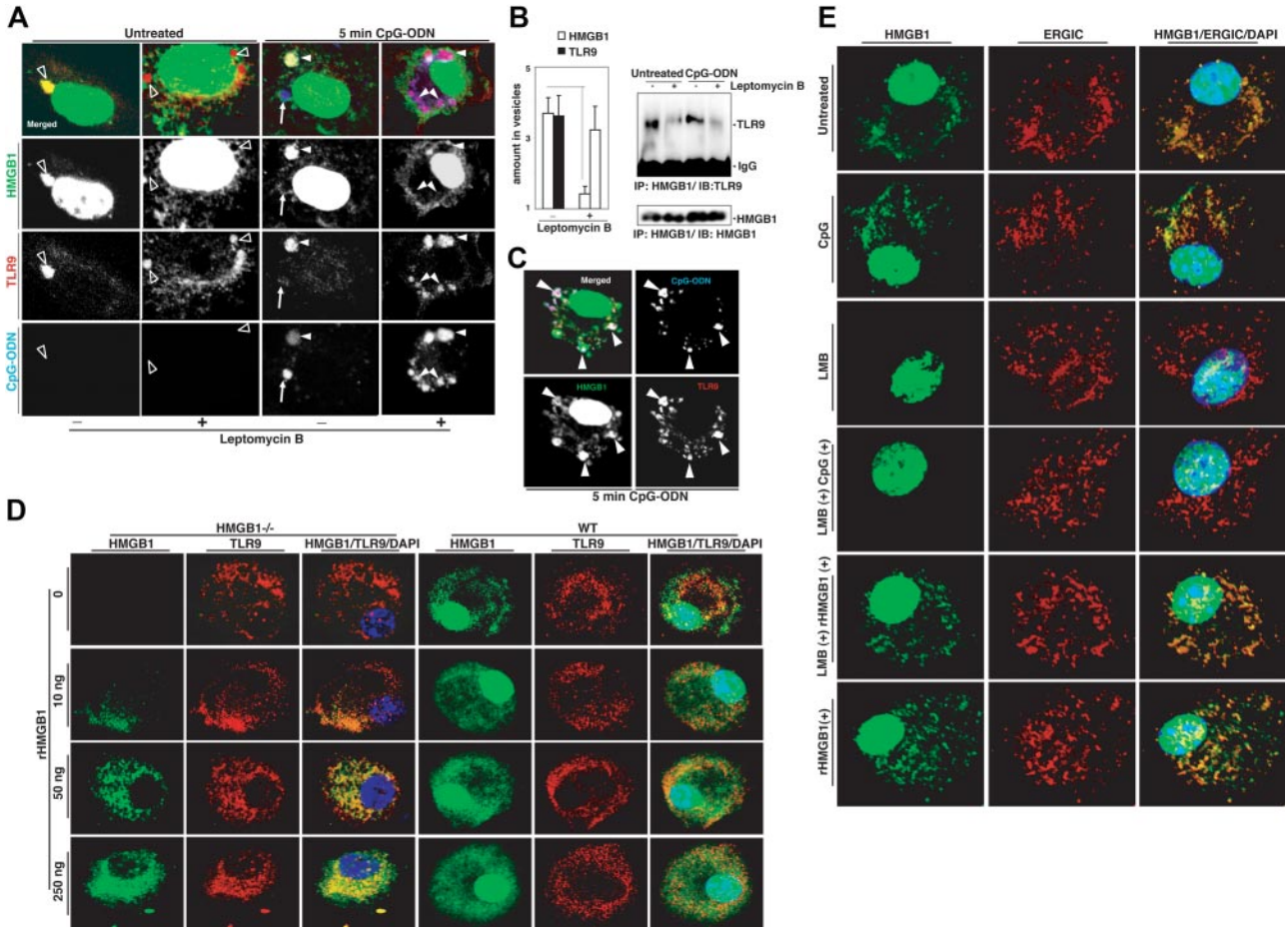

Figure 5. HMGB1 in vesicles is from the nucleus. (A) LMB inhibits HMGB1 translocation into TLR9-containing vesicles. BMDMs were incubated in the presence or absence of 20 ng/mL LMB for 45 minutes, followed by treatment with CpG-ODN-Cy5 (1018, 5 μg/mL). △ indicate HMGB1-containing vesicles; ▲, CpG-DNA-containing vesicles; and ↑, early CpG-DNA-containing vesicle prior to acquisition by HMGB1/TLR9-containing vesicles. (B) Quantitative analysis of the fluorescence of HMGB1 and TLR9 within vesicles over background fluorescence in BMDMs treated with or without 20 ng/mL LMB for 45 minutes (means ± SEM, n = 35, $^{**}P < .001$, Student *t* test). (C) LMB impairs the formation of the TLR9-HMGB1 complex. HMGB1 was immunoprecipitated from lysates of WEHI-231 cells that were treated with 20 ng/mL LMB for 45 minutes prior to stimulation with CpG-ODN (10 μg/mL) for 30 minutes. (D) Exogenously added rHMGB1 can restore the presence of HMGB1 in the vesicles. rHMGB1 (25 ng/mL) was incubated with CpG-ODN-Cy5 (1018, 5 μg/mL) for 60 minutes and added to BMDMs treated with 20 ng/mL LMB for 45 minutes. ▲ indicate TLR9 extensively colocalized with CpG-DNA/HMGB1-containing vesicles. (E) Addition of rHMGB1 increases colocalization of HMGB1 with TLR9. Different amounts of rHMGB1 as indicated were incubated with wt and HMGB1-deficient macrophages (IFLMDs) for 10 minutes. Colocalization of TLR9 with HMGB1 was determined. (F) Translocation of HMGB1 into ERGIC-53–containing vesicles can be blocked by LMB and restored by exogenous rHMGB1. BMDMs were starved for 3 hours and then treated with LMB or left untreated for 60 minutes. Cells were incubated with CpG-ODN (10 μg/mL) or rHMBG1 (50 ng/mL) for 10 minutes in the presence or absence of LMB.

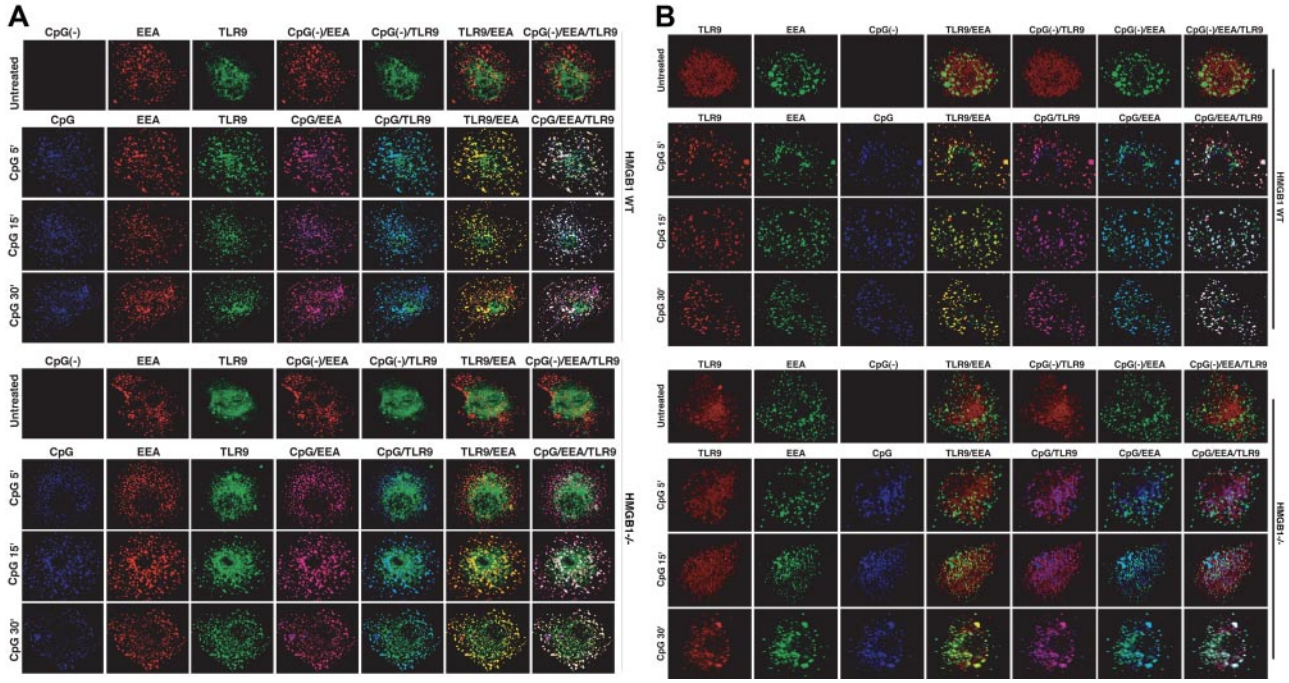

Figure 6. HMGB1 accelerates early endosomal translocation of TLR9 in macrophages in response to CpG-ODN. (A,B) Wt (top panels) and HMGB1-deficient (bottom panels) IFLDMs (A) or PFLDMs (B) were treated with CpG-ODN-Cy5 (1018, 5 μg/mL) for 0, 5, 15, or 30 minutes. Cells were fixed, permeabilized, and stained with anti-TLR9/FITC and anti-EEA1/rhodamine. Confocal images were acquired by indirect immunofluorescence.

TLR9 vesicles by 2 routes: from the nuclear pool and from the extracellular milieu.

HMGB1 is involved in the translocation of TLR9 to early endosomes in response to CpG-ODN

The redistribution of TLR9 from the ER to early endosomes is essential for TLR9 activation by CpG-DNA.[11] As our experimental results demonstrate that HMGB1 preassociates with TLR9 in quiescent cells, we postulated that HMGB1 is involved in the TLR9 translocation process. Thus, we investigated the relationship between HMGB1, TLR9, and the early endosome marker EEA1[11] in both wt and HMGB1-deficient macrophages (characterized in Figure 7A) by surveying 200 cells in each condition (Figure 6). Consistent with previous results,[11] most TLR9 and EEA1 did not colocalize in quiescent wt and HMGB1-deficient cells (untreated, Figure 6A,B). Surprisingly, CpG-ODN uptake and colocalization of CpG-ODN with EEA1 in both wt and HMGB1-deficient cells were comparable (CpG vs CpG/EEA1, Figure 6A,B), suggesting that the lack of HMGB1 has no effect on CpG-DNA endocytosis. Importantly, in wt macrophages most TLR9 was redistributed and colocalized with EEA1 after 5 to 15 minutes of CpG-ODN treatment, and then deassociated from early endosomes after 30 minutes. There was little colocalization of TLR9 with EEA1 in HMGB1-deficient cells 5 to 15 minutes following CpG-ODN stimulation (Figure 6A,B), but there was increased colocalization of TLR9 with EEA1 at 30 minutes. Thus, the kinetics of TLR9 colocalization with EEA1 in HMGB1-deficient cells is delayed. This is further supported by our pharmacological results (Figure S3), as the depletion of cytoplasmic HMGB1 in wt BMDMs by LMB largely impaired the association of HMGB1 with TLR9, retained TLR9 in ER-like structures for up to 15 minutes following CpG-ODN stimulation, and postponed the colocalization of TLR9 with EEA1. Taken together, our results suggest that HMGB1 does not affect the uptake of CpG-ODN or its entry into early endosomes, but accelerates TLR9 redistribution to early endosomes in response to CpG-ODN.

HMGB1-deficient cells show defective cytokine responses to CpG-ODN

Because HMGB1-null mice die postnatally,[24] we were unable to use them to assess cellular responses to CpG-ODN in vivo. Thus, we sought to create chimeras by transplanting fetal liver cells (FLCs) isolated from mouse embryos into mice irradiated lethally with ^{137}Cs. Unexpectedly, HMGB1-deficient FLCs failed to rescue the irradiated mice, due to a yet unidentified reason (Chu et al, unpublished data). Then we decided to derive DCs and macrophages from primary FLCs (PFLCs) or FLCs immortalized by transfection with HoxB4 (IFLCs). Both IFLCs and PFLCs were able to differentiate into DCs (IFLDCs and PFLDCs, respectively), as determined by cell surface expression of CD11b and CD11c, or macrophages (IFLDMs and PFLDMs, respectively), as determined by CD11b and F4/80 (Figure 7A).

Both wt and HMGB1-deficient IFLDCs expressed equal amounts of TLR9 (Figure 7B). Importantly, both wt and HMGB1-deficient IFLDCs demonstrated a comparable ability to uptake CpG-ODN in a dose-independent manner (Figure 7C). This is consistent with observations described previously (Figure 6A,B).

Next, we determined the cytokine response to CpG-DNA in HMGB1-deficient cells. Wt IFLDMs showed a robust IL-6 induction in response to CpG-ODN with a saturation threshold at 100 nM CpG-ODN. Conversely, HMGB1-deficient IFLDMs produced only minimal amounts of IL-6 even at 1 μM CpG-ODN (Figure 7D). Wt and HMGB1-deficient IFLDMs responded comparably with LPS and PGN.

HMGB1-deficient IFLDCs exhibited a reduced IL-6, TNFα, and IL-12 response to CpG-ODN (Figure 7E). The reduction of cytokines in *Hmgb1*$^{-/-}$ IFLDCs was most visible at lower

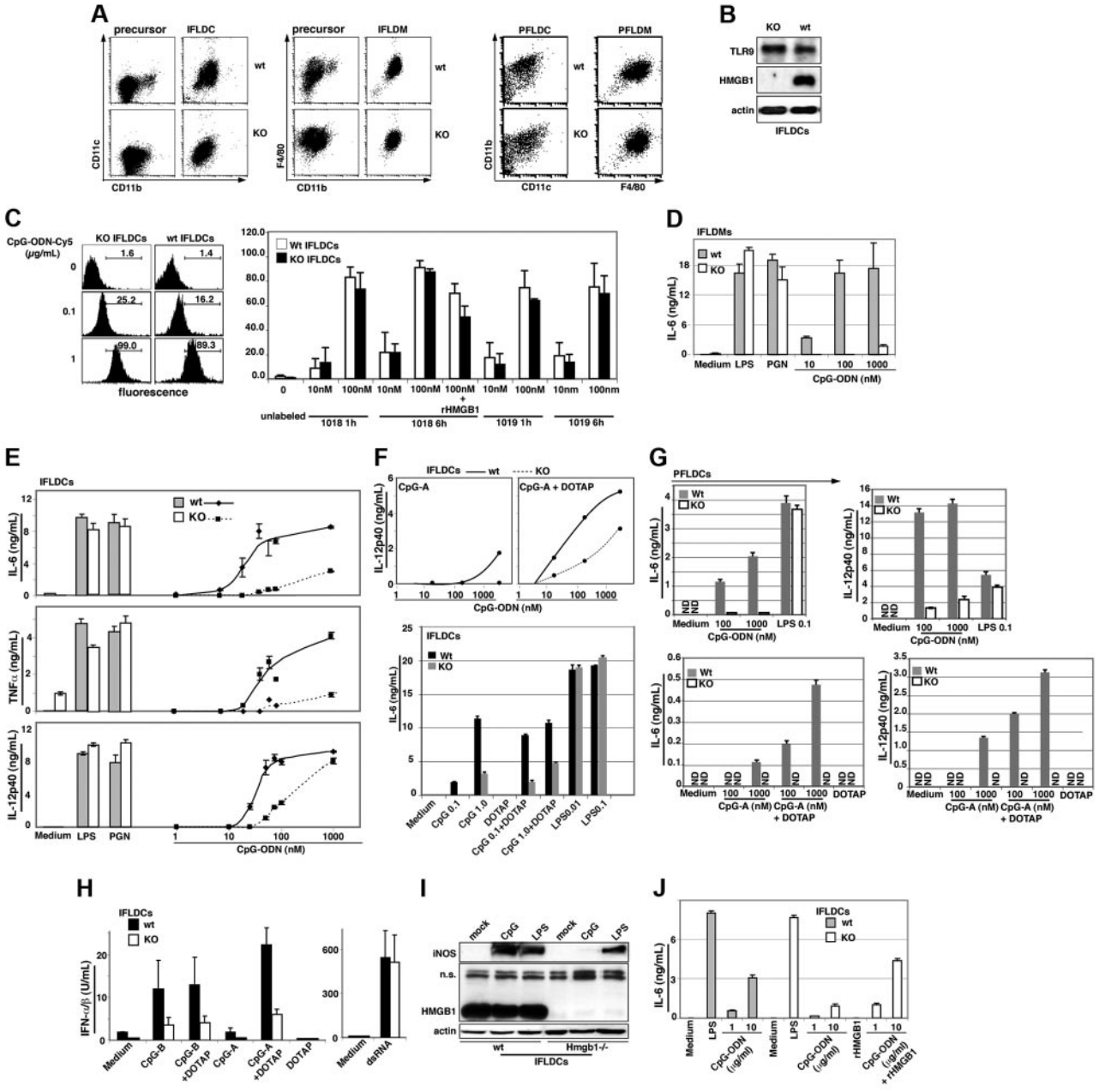

Figure 7. Impaired CpG-ODN responses in *Hmgb1*$^{-/-}$ cells. (A) Wt and *Hmgb1*$^{-/-}$ immortalized or primary hematopoietic progenitor cells (HPCs) expressed the DC markers CD11b and CD11c following incubation with GM-CSF for 7 days, or expressed CD11b and F4/80 after culture with macrophage medium for 10 days. Although HPCs are uniformly round and nonadherent, following differentiation they become adherent and acquire a macrophage-like morphology. (IFLDCs indicates DCs derived from immortalized fetal liver. HPCs; PFLDCs, DCs derived from primary fetal liver HPCs.) (B) Protein levels of HMGB1, TLR9, and actin in wt and *Hmgb1*$^{-/-}$ IFLDCs. (C) Wt and *Hmgb1*$^{-/-}$ IFLDCs endocytosed comparable levels of CpG-ODN or GpG-ODN. Cells were treated with CpG-ODN-Cy5 (0.1 or 1.0 μg/mL for 1 hour, left panel), CpG-ODN-Cy5 (1018, 10 or 100 nM), or GpG-ODN-Cy5 (1019, 10 or 100 nM) for the indicated time points (right panel), and then subjected to FACS analysis. (D) Wild-type and *Hmgb1*$^{-/-}$ IFLDMs were seeded at 1×10^5/well in a 96-well plate (in triplicate) and treated with CpG-ODN (1018, 10 to 1000 nM), LPS (0.1 μg/mL), or PGN (10 μg/mL). After 24 hours, IL-6 secretion was assessed by ELISA (bars represent the average of triplicates ± SD). Experiments were replicated 3 times. (E) Wt and *Hmgb1*$^{-/-}$ IFLDCs were seeded at 1×10^5/well in a 96-well plate (in triplicate) and treated with CpG-ODN (1018, 1 to 1000 nM), LPS (0.1 μg/mL), or PGN (10 μg/mL). After 24 hours, IL-6, IL-12, and TNFα secretion was assessed by ELISA (bars represent the average of triplicates ± SD). Experiments were replicated 5 times. (F) Wt and *Hmgb1*$^{-/-}$ IFLDCs were seeded at 1×10^5/well in a 96-well plate (in triplicate) and treated with CpG-A (2216, 1 to 1000 nM, top panel) or CpG-ODN (1018, 0.1 or 1.0 μg/mL, bottom panel) in the presence or absence of DOTAP (10 μg/mL), or LPS (0.01 or 0.1 μg/mL, bottom panel), or left untreated. After 24 hours, IL-12 (top panel) or IL-6 (bottom panel) secretion was assessed by ELISA (bars represent the average of triplicates ± SD). (G) Wt and *Hmgb1*$^{-/-}$ PFLDCs were seeded at 0.8×10^5/well in a 96-well plate (in triplicate) and treated with CpG-ODN (1018, 100 or 1000 nM) or CpG-A (2216, 100 or 1000 nM) in the presence or absence of DOTAP (10 μg/mL), or LPS (0.1 μg/mL), or left untreated. After 24 hours, IL-6 and IL-12 secretion was assessed by ELISA (bars represent the average of triplicates ± SD). ND: not detected. (H) Wt and *Hmgb1*$^{-/-}$ IFLDCs were treated with CpG-B (1018, 10 μg/mL), CpG-A (2216, 3.3 μg/mL), and poly(I:C) (10 μg/mL) in the presence or absence of DOTAP (10 μg/mL) for 24 hours. Type 1 IFN bioactivity in supernatant samples was detected by a biologic assay against vesicular stomatitis virus.[45] (I) Whole-cell lysates were prepared at 16 hours after treatment with CpG-ODN (1018, 10 μg/mL) or LPS (1 μg/mL) and the levels of iNOS, HMGB1, and actin were determined by IB. (n.s. = nonspecific band.) (J) Exogenous rHMGB1 restored cytokine production by *Hmgb1*$^{-/-}$ IFLDCs in response to CpG-ODN. rHMGB1 (rH1, 0.2 μg/mL) was incubated in the presence or absence of CpG-ODN (1018) for 15 minutes. Wt and *Hmgb1*$^{-/-}$ IFLDCs were treated with CpG-ODN (1018, 1 or 10 μg/mL) ± rHMGB1, LPS (0.1 μg/mL), or rH1 alone, or left untreated for 24 hours, and the levels of secreted IL-6 were determined by ELISA (bars represent the average of triplicates ± SD).

concentrations of CpG-ODN. Interestingly, the IL-12 response to CpG-ODN at 1 μM in HMGB1-deficient IFLDCs was close to, but still less than, that of wt controls. Both wt and HMGB1-deficient IFLDCs responded to LPS and PGN equally (Figure 7E). The defective response to CpG-ODN was reproducible in 3 independently derived pools of HMGB1-deficient IFLCs (data not shown). Unlike class B CpG-ODN 1018 (CpG-B), in response to class *A* CpG-ODN (CpG-A) wt, but not *Hmgb1*$^{-/-}$, IFLDCs secreted IL-12 (Figure 7F top panel). Lower levels of IL-12 were produced by *Hmgb1*$^{-/-}$ compared with wt IFLDCs when stimulated with CpG-A in the presence of the cationic lipid 1,2-dioleoyloxy-3-trimethylammonium-propane (DOTAP) (Figure 7F top panel). A similar phenomenon occurred for IL-6 when cells were treated with CpG-A and DOTAP, whereas CpG-A alone failed to induce IL-6 (Figure 7F bottom panel). Cellular activation triggered by CpG-ODNs in the presence of DOTAP was sensitive to quinacrine and therefore dependent on TLR9 (data not shown).

Consistently, the defects in HMGB1-deficient IFLDCs were also observed in HMGB1-deficient PFLDCs. HMGB1 deficiency led to a severe defect in the IL-6 and IL-12 response to CpG-ODN even at 1 μM (Figure 7G). In addition, regardless of the presence or absence of DOTAP, CpG-A failed to induce a detectable level of IL-6 and IL-12 production in HMGB1- deficient PFLDCs (Figure 7G). These experimental results suggest a critical role for HMGB1 in the cytokine response to CpG-DNA.

To further investigate a role of HMGB1 in the activation of innate immunity by CpG-DNA, we tested the ability of wt and *Hmgb1*$^{-/-}$ IFLDCs to secrete IFNα/β in response to CpG-A and CpG-B.[47] Wt IFLDCs produced low but significant levels of IFNα/β when treated with CpG-B irrespective of DOTAP presence, whereas CpG-A was stimulatory only in the presence of DOTAP (Figure 7H). Wt IFLDCs produced 2- to 3-fold higher levels of type I IFNs compared with *Hmgb1*$^{-/-}$ cells in response to CpG-DNAs. As a control, poly(I:C) triggered a potent release of IFNα/β by both wt and HMGB1-deficient cells.

In addition, we assessed the expression of inducible nitric oxide synthase (iNOS),[48] which can be induced by CpG-DNA and other TLR agonists.[49-51] CpG-ODN completely failed to induce iNOS expression in HMGB1-deficient IFLDCs (Figure 7I), in contrast to wt IFLDCs. However, both wt and HMGB1-deficient IFLDCs exhibited a similar iNOS response to LPS (Figure 7I).

Finally, we determined whether exogenously supplied HMGB1 could compensate for the lack of endogenous HMGB1 in the cytokine response to CpG-DNA. When HMGB1-deficient IFLDCs were provided with exogenous HMGB1, the IL-6, IL-12, and TNFα response to CpG-ODN was restored (Figure 7J and data not shown).

Taken together, these experiments indicate that HMGB1 is required for optimal cytokine and iNOS responses to CpG-DNA.

Discussion

TLR9 activation by microbial CpG-DNA and CpG-ODNs in innate immune cells induces the secretion of cytokines, leading to elimination of microbial pathogens and activation of the adaptive immunity.[1,2] It has been suggested that CpG-DNAs are endocytosed into endosomal compartments where they engage the intracellular TLR9, resulting in MyD88 recruitment and the subsequent immune response.[7-10] However, the precise physiological process leading to TLR9 activation by CpG-DNA remains unclear. In this study, we describe a novel role for HMGB1 as an important regulator in this process.

Our findings demonstrate that HMGB1, which binds CpG-ODNs, interacts with TLR9 within vesicles, probably belonging to the ERGIC, of quiescent macrophages. This interaction precedes CpG-ODN uptake, and both intracellular HMGB1 from the nucleus and extracellular HMGB1 from the medium can be recruited to interact with TLR9. Immune cells lacking HMGB1 show a delayed redistribution of TLR9 into the early endosomes and an impaired cytokine response to CpG-ODN. The latter defect was restored when exogenous HMGB1 was supplied. Thus, our experimental data suggest that HMGB1 plays an important role in regulating the process of TLR9 activation by CpG-DNA. Recently, a similar conclusion was reached independently by Coyle's group (Tian et al[52]).

Most cytokine responses to CpG-DNA are undetectable in TLR9-null cells[7]; however, HMGB1-deficient cells exhibited partial responses. Most notably, the IL-12 response to high doses of CpG-ODN in HMGB1-deficient IFLDCs was lower than, but close to, that of wt cells. Interestingly, when examined in primary fetal liver progenitor cell-derived DCs (PFLDCs), the IL-12 response to CpG-ODNs even at 1 μM remains largely impaired in HMGB1-deficient PFLDCs, underscoring a critical role for HMGB1 in the cytokine response to CpG-DNA. Nevertheless, the partial penetrance of the *Hmgb1* mutation suggests a role of HMGB1 as a cofactor that modulates TLR9 activation. This cofactor is not as essential as TLR9 in the activation of the CpG-DNA pathway, but lowers the effective concentration of CpG-DNA necessary for triggering cellular responses by engaging CpG-DNA, interacting with TLR9, and facilitating the recognition of CpG-DNA.

TLR9 resides in the ER and its activation requires CpG-ODN endocytosis and the subsequent early endosomal acidification.[35] Our findings demonstrate that TLR9/HMGB1 vesicles not only reside in the ER, but also colocalize with markers of the ERGIC and the Golgi in quiescent cells. We observed that the lumen of TLR9/HMGB1 vesicles is acidic prior to CpG-DNA accumulation. This is consistent with the ERGIC environment where a vacuolar H^+-ATPase pump is active.[53,54]

MD2, a coreceptor for TLR4, plays an important role in LPS recognition and contributes to the cell surface localization of TRL4.[55,56] The loss of MD2 results in TLR4 accumulation in the Golgi compartment.[56] Similarly, in HMGB1-deficient macrophages or cytoplasmic HMGB1-depleted BMDMs, TLR9 is retained in the ER or the ERGIC following CpG-ODN treatment, whereas HMGB1 deficiency has no apparent effect on CpG-ODN uptake or its entry into early endosomes. Our results show that preassociation of HMGB1 with CpG-ODN leads to earlier detection of CpG-ODNs in the TLR9 immune complex (Figure 2). Thus, our data further suggest that HMGB1 contributes to the redistribution of TLR9 to early endosomes.

HMGB1 is considered a nonspecific single/double-stranded DNA-binding protein,[13] whereas our data show that HMGB1 has some preference for binding CpG-ODNs over GpC/GpG-ODNs. It is known that a simple inversion of the "CpG" in CpG-ODN to the "GpC" or a subtle substitution of the "CpG" with the "GpG," which largely impairs CpG-ODN′s biologic activity, also affects the ability to form hairpins or oligo-dimer structures.[31,57,58] However, it is unclear whether HMGB1 has some preferences to bind such structures. To resolve this, more detailed structure-activity studies are needed in the future.

HMGB1 is secreted from immune cells upon challenge with a variety of stimuli. Whether CpG-DNA induces secretion of HMBG1 from immune cells is controversial.[32,33] Our data demonstrate that

CpG-ODN triggers the release of HMGB1 from immune cells in a matter of minutes. Quick release of HMGB1 may accelerate the recognition of CpG-DNA and sensitize other immune cells to CpG-DNA, by both autocrine and paracrine signaling. Moreover, other stimuli that lead to HMGB1 secretion could also potentially sensitize cells to CpG-ODNs.

How does secreted HMGB1 enhance cytokine production in response to CpG-ODN? One possibility is that HMGB1 increases CpG-ODN uptake. Conversely, our experimental results indicate that the uptake of CpG-ODNs by cells was somewhat decreased in the presence of HMGB1, and was not apparently affected by the depletion or deletion of HMGB1. Another possibility is that HMGB1 uses its potential receptors such as TLR2 and TLR4[19,59,60] to synergize or cross-talk with TLR9. However, the HMGB1-enhanced cytokine response we have shown here is CpG-DNA specific, as HMGB1 alone had minimal effects, and TLR2-deficient and TLR4 mutant cells responded comparably with wt cell when stimulated with CpG-ODN and HMGB1 in producing IL-6. Moreover, coincubation of HMGB1 with LPS or PGN failed to enhance cytokine secretion. Thus, we suggest that HMGB1 accelerates and increases the recognition of CpG-ODN by TLR9. We showed that loss of HMGB1 delayed the early endosomal translocation of TLR9 (Figure 6) and preassociation of HMGB1 with CpG-ODNs led to the earlier detection of CpG-ODNs in the TLR9 immune complex (Figure 2G).

CpG-ODN and HMGB1 can give rise to a reciprocal feedback cycle: innate immune cells secrete HMGB1 in response to CpG-DNA, and HMGB1 sensitizes innate immune cells to CpG-DNA. Our data demonstrate that macrophages can prime this cycle in the absence of preexisting extracellular HMGB1. They assemble vesicular organelles where a small pool of HMGB1 that is released from the nucleus preassociates with TLR9. Following stimulation, CpG-DNA-rich endosomes acquire HMGB1 and TLR9 from these vesicles, leading to TLR9 activation. The defect in the CpG-DNA response due to the lack of HMGB1 is relieved by addition of appropriate forms of exogenous HMGB1.

In conclusion, our identification of HMGB1 as an important modulator of TLR9 activation by CpG-DNA provides a link between endogenous nuclear proteins and the principal innate immune sensors of mammals.

Acknowledgments

This work was supported by grants from the NIH to W.-M.C. (AI 54128) and C.A.B. (AI 55677), from COBRE and DOD (PR054819) to W.-M.C., and from Associazione Italiana Ricerca sul Cancro to M.E.B. J.L. was supported by the NDSE predoctoral fellowship. W.-M.C. is a scholar of Leukemia and Lymphoma Society.

We are grateful to Dr Shizuo Akira for providing TLR2-, TLR9-, and MyD88-deficient mice, Dr Dominic van Essen for the Hox4 vector, and to Dr Lorenza Ronfani and the CFCM staff for producing *Hmgb1*$^{-/-}$ embryos. We thank Drs Sankar Ghosh and Anlin Lin and Mr Matthew Riolo for their critical discussion, and Dr Enrico Bucci for useful suggestions. We also thank Drs Xiao Peng, Seung-Hwan Lee, Charles Vaslet, Mingwei Zhu, and Stephanie Beall for their technical assistance.

Authorship

Contribution: S.I., A.-M.D., and W.-M.C. executed all experiments except those indicated; X.W. identified the relationship between HMGB1/TLR9, early endosomes, and the ERGIC; C.D. and G.M. studied HMGB1/ODN binding; G.S. generated *Hmgb1*$^{-/-}$ cells; J.L., C.A.B., and G.S.Y. characterized HPCs, CpG-ODN uptake, and IFNα/β production; Y.W. characterized *Hmgb1*$^{-/-}$ cells and CpG-ODN activation; W.-M.C., M.E.B, H.W., and G.S.Y. provided intellectual input.

Conflict-of-interest disclosure: The authors declare no competing financial interests.

Correspondence: Wen-Ming Chu, Box G-B6, Brown University, 171 Meeting St, Providence, RI 02912; email: wen-ming_chu@brown.edu.

References

1. Akira S, Takeda K, Kaisho T. Toll-like receptors: critical proteins linking innate and acquired immunity. Nat Immunol. 2001;2:675-680.
2. Takeda K, Kaisho T, Akira S. Toll-like receptors. Annu Rev Immunol. 2003;21:335-376.
3. Karlin S, Doerfler W, Cardon LR. Why is CpG suppressed in the genomes of virtually all small eukaryotic viruses but not in those of large eukaryotic viruses? J Virol. 1994;68:2889-2897.
4. Cardon LR, Burge C, Clayton DA, Karlin S. Pervasive CpG suppression in animal mitochondrial genomes. Proc Natl Acad Sci U S A. 1994;91:3799-3803.
5. Razin A, Friedman J. DNA methylation and its possible biological roles. Prog Nucleic Acid Res Mol Biol. 1981;25:33-52.
6. Stacey KJ, Young GR, Clark F, et al. The molecular basis for the lack of immunostimulatory activity of vertebrate DNA. J Immunol. 2003;170:3614-3620.
7. Hemmi H, Takeuchi O, Kawai T, et al. A Toll-like receptor recognizes bacterial DNA. Nature. 2000;408:740-745.
8. Bauer M, Redecke V, Ellwart JW, et al. Bacterial CpG-DNA triggers activation and maturation of human CD11c-, CD123+ dendritic cells. J Immunol. 2001;166:5000-5007.
9. Ahmad-Nejad P, Hacker H, Rutz M, Bauer S, Vabulas RM, Wagner H. Bacterial CpG-DNA and lipopolysaccharides activate Toll-like receptors at distinct cellular compartments. Eur J Immunol. 2002;32:1958-1968.
10. Bauer S, Kirschning CJ, Hacker H, et al. Human TLR9 confers responsiveness to bacterial DNA via species-specific CpG motif recognition. Proc Natl Acad Sci U S A. 2001;98:9237-9242.
11. Latz E, Schoenemeyer A, Visintin A, et al. TLR9 signals after translocating from the ER to CpG DNA in the lysosome. Nat Immunol. 2004;5:190-198.
12. Hacker H, Vabulas RM, Takeuchi O, Hoshino K, Akira S, Wagner H. Immune cell activation by bacterial CpG-DNA through myeloid differentiation marker 88 and tumor necrosis factor receptor-associated factor (TRAF)6. J Exp Med. 2000;192:595-600.
13. Agresti A, Bianchi ME. HMGB proteins and gene expression. Curr Opin Genet Dev. 2003;13:170-178.
14. Bianchi ME, Agresti A. HMG proteins: dynamic players in gene regulation and differentiation. Curr Opin Genet Dev. 2005;15:496-506.
15. Dumitriu IE, Baruah P, Manfredi AA, Bianchi ME, Rovere-Querini P. HMGB1: guiding immunity from within. Trends Immunol. 2005;26:381-387.
16. Scaffidi P, Misteli T, Bianchi ME. Release of chromatin protein HMGB1 by necrotic cells triggers inflammation. Nature. 2002;418:191-195.
17. Palumbo R, Sampaolesi M, De Marchis F, et al. Extracellular HMGB1, a signal of tissue damage, induces mesoangioblast migration and proliferation. J Cell Biol. 2004;164:441-449.
18. Park JS, Svetkauskaite D, He Q, et al. Involvement of toll-like receptors 2 and 4 in cellular activation by high mobility group box 1 protein. J Biol Chem. 2004;279:7370-7377.
19. Tsung A, Sahai R, Tanaka H, et al. The nuclear factor HMGB1 mediates hepatic injury after murine liver ischemia-reperfusion. J Exp Med. 2005;201:1135-1143.
20. Chu W, Gong X, Li Z, et al. DNA-PKcs is required for activation of innate immunity by immunostimulatory DNA. Cell. 2000;103:909-918.
21. Wang H, Bloom O, Zhang M, et al. HMG-1 as a late mediator of endotoxin lethality in mice. Science. 1999;285:248-251.
22. Wang H, Yang H, Tracey KJ. Extracellular role of HMGB1 in inflammation and sepsis. J Intern Med. 2004;255:320-331.
23. Dragoi AM, Fu X, Ivanov S, et al. DNA-PKcs, but not TLR9, is required for activation of Akt by CpG-DNA. EMBO J. 2005;24:779-789.
24. Calogero S, Grassi F, Aguzzi A, et al. The lack of chromosomal protein Hmg1 does not disrupt cell

growth but causes lethal hypoglycaemia in newborn mice. Nat Genet. 1999;22:276-280.

25. Zhang Y, Wang Y, Ogata M, Hashimoto S, Onai N, Matsushima K. Development of dendritic cells in vitro from murine fetal liver-derived lineage phenotype-negative c-kit(+) hematopoietic progenitor cells. Blood. 2000;95:138-146.
26. Verthelyi D, Zeuner RA. Differential signaling by CpG DNA in DCs and B cells: not just TLR9. Trends Immunol. 2003;24:519-522.
27. Lee SW, Song MK, Baek KH, et al. Effects of a hexameric deoxyriboguanosine run conjugation into CpG oligodeoxynucleotides on their immunostimulatory potentials. J Immunol. 2000;165: 3631-3639.
28. Wu CCN, Lee J, Raz E, Corr M, Carson DA. Necessity of oligonucleotide aggregation for Toll-like receptor 9 activation. J Biol Chem. 2004;279: 33071-33078.
29. Marshall JD, Fearon K, Abbate C, et al. Identification of a novel CpG DNA class and motif that optimally stimulate B cell and plasmacytoid dendritic cell functions. J Leukoc Biol. 2003;73:781-792.
30. Sato Y, Roman M, Tighe H, et al. Immunostimulatory DNA sequences necessary for effective intradermal gene immunization. Science. 1996;273: 352-354.
31. Krieg AM, Yi AK, Matson S, et al. CpG motifs in bacterial DNA trigger direct B-cell activation. Nature. 1995;374:546-549.
32. Dumitriu IE, Baruah P, Bianchi ME, Manfredi AA, Rovere-Querini P. Requirement of HMGB1 and RAGE for the maturation of human plasmacytoid dendritic cells. Eur J Immunol. 2005;35:2184-2190.
33. Jiang W, Li J, Gallowitsch-Puerta M, Tracey KJ, Pisetsky DS. The effects of CpG DNA on HMGB1 release by murine macrophage cell lines. J Leukoc Biol. 2005;78:930-936.
34. Yi AK, Hornbeck P, Lafrenz DE, Krieg AM. CpG DNA rescue of murine B lymphoma cells from anti-IgM-induced growth arrest and programmed cell death is associated with increased expression of c-myc and bcl-xL. J Immunol. 1996;157: 4918-4925.
35. Leifer CA, Kennedy MN, Mazzoni A, Lee C, Kruhlak MJ, Segal DM. TLR9 is localized in the endoplasmic reticulum prior to stimulation. J Immunol. 2004;173:1179-1183.
36. Macfarlane DE, Manzel L. Antagonism of immunostimulatory CpG-oligodeoxynucleotides by quinacrine, chloroquine, and structurally related compounds. J Immunol. 1998;160:1122-1131.
37. Manzel L, Strekowski L, Ismail FM, Smith JC, Macfarlane DE. Antagonism of immunostimulatory CpG-oligodeoxynucleotides by 4-aminoquinolines and other weak bases: mechanistic studies. J Pharmacol Exp Ther. 1999;291:1337-1347.
38. Blott EJ, Griffiths GM. Secretory lysosomes. Nat Rev Mol Cell Biol. 2002;3:122-131.
39. Appenzeller-Herzog C, Roche AC, Nufer O, Hauri HP. pH-induced conversion of the transport lectin ERGIC-53 triggers glycoprotein release. J Biol Chem. 2004;279:12943-12950.
40. Eskelinen EL, Tanaka Y, Saftig P. At the acidic edge: emerging functions for lysosomal membrane proteins. Trends Cell Biol. 2003;13:137-145.
41. Schweizer A, Fransen JA, Bachi T, Ginsel L, Hauri HP. Identification, by a monoclonal antibody, of a 53-kD protein associated with a tubulovesicular compartment at the cis-side of the Golgi apparatus. J Cell Biol. 1988;107:1643-1653.
42. Marra P, Maffucci T, Daniele T, et al. The GM130 and GRASP65 Golgi proteins cycle through and define a subdomain of the intermediate compartment. 2001;3:1101-1113.
43. Bonaldi T, Talamo F, Scaffidi P, et al. Monocytic cells hyperacetylate chromatin protein HMGB1 to redirect it towards secretion. EMBO J. 2003;22: 5551-5560.
44. Fornerod M, Ohno M, Yoshida M, Mattaj IW. CRM1 is an export receptor for leucine-rich nuclear export signals. Cell. 1997;90:1051-1060.
45. Fukuda M, Asano S, Nakamura T, et al. CRM1 is responsible for intracellular transport mediated by the nuclear export signal. Nature. 1997;390:308-311.
46. Dalod M, Salazar-Mather TP, Malmgaard L, et al. Interferon alpha/beta and interleukin 12 responses to viral infections: pathways regulating dendritic cell cytokine expression in vivo. J Exp Med. 2002;195:517-528.
47. Kerkmann M, Rothenfusser S, Hornung V, et al. Activation with CpG-A and CpG-B oligonucleotides reveals two distinct regulatory pathways of type I IFN synthesis in human plasmacytoid dendritic cells. J Immunol. 2003;170:4465-4474.
48. Bogdan C. Nitric oxide and the immune response. Nat Immunol. 2001;2:907-916.
49. Ghosh DK, Misukonis MA, Reich C, Pisetsky DS, Weinberg JB. Host response to infection: the role of CpG DNA in induction of cyclooxygenase 2 and nitric oxide synthase 2 in murine macrophages. Infect Immun. 2001;69:7703-7710.
50. Frances R, Munoz C, Zapater P, et al. Bacterial DNA activates cell mediated immune response and nitric oxide overproduction in peritoneal macrophages from patients with cirrhosis and ascites. Gut. 2004;53:860-864.
51. He H, Crippen TL, Farnell MB, Kogut MH. Identification of CpG oligodeoxynucleotide motifs that stimulate nitric oxide and cytokine production in avian macrophage and peripheral blood mononuclear cells. Dev Comp Immunol. 2003;27:621-627.
52. Tian J, Avalos AM, Mao SY, et al. Toll-like receptor 9-dependent activation by DNA-containing immune complexes is mediated by HMGB1 and RAGE. Nat Immunol. 2007;8:487-496.
53. Ying M, Flatmark T, Saraste J. The p58-positive pre-golgi intermediates consist of distinct subpopulations of particles that show differential binding of COPI and COPII coats and contain vacuolar H(+)-ATPase. J Cell Sci. 2000;113: 3623-3638.
54. Palokangas H, Ying M, Vaananen K, Saraste J. Retrograde transport from the pre-Golgi intermediate compartment and the Golgi complex is affected by the vacuolar H+-ATPase inhibitor bafilomycin A1. Mol Biol Cell. 1998;9:3561-3578.
55. Shimura H, Nitahara A, Ito A, Tomiyama K, Ito M, Kawai K. Up-regulation of cell surface Toll-like receptor 4-MD2 expression on dendritic epidermal T cells after the emigration from epidermis during cutaneous inflammation. J Dermatol Sci. 2005;37:101-110.
56. Nagai Y, Akashi S, Nagafuku M, et al. Essential role of MD-2 in LPS responsiveness and TLR4 distribution. Nat Immunol. 2002;3:667-672.
57. Yamamoto S, Yamamoto T, Kataoka T, Kuramoto E, Yano O, Tokunaga T. Unique palindromic sequences in synthetic oligonucleotides are required to induce IFN [correction of INF] and augment IFN-mediated [correction of INF] natural killer activity. J Immunol. 1992;148:4072-4076.
58. Sonehara K, Saito H, Kuramoto E, Yamamoto S, Yamamoto T, Tokunaga T. Hexamer palindromic oligonucleotides with 5′-CG-3′ motif(s) induce production of interferon. J Interferon Cytokine Res. 1996;16:799-803.
59. Lotze MT, Tracey KJ. High-mobility group box 1 protein (HMGB1): nuclear weapon in the immune arsenal. Nat Rev Immunol. 2005;5:331-342.
60. Yu M, Wang H, Ding A, et al. HMGB1 signals through toll-like receptor (TLR) 4 and TLR2. Shock. 2006;26:174-179.